AIAA Paper 97-0548, 35th Aerospace Sciences Meeting

Reduction of Fluctuations over Swept Wings Using Passive and Active Mini-Fences

M. A. Klein*, W. K. Lentz† and N. M. Komerath‡
School of Aerospace Engineering
Georgia Institute of Technology
Atlanta, GA 30332-0150

ABSTRACT

Passive and active surface devices are used to modify the narrow-band velocity fluctuations over a 59.3 degree delta wing at high angles of attack. Previous work has traced these fluctuations to counter-rotating structures in the shear layer below the post-burst vortex. Small vertical fences placed near the point of origin of the fluctuations attenuate the peak spectral energy by as much as 78%. The lift and drag are shown to be unaffected. Fences placed at other locations and orientations show various levels of suppression and amplification. The most effective fence height, position, and orientation for attenuation at 25 deg. angle of attack are identified. An active fence and a ramp modulated at the fluctuation frequency show attenuation corresponding to the effective duty cycle of deployment in a given range of the shear layer. It is seen that the fences must extend well beyond the surface boundary layer to be effective, but extending into the central region of the flow is ineffective, further proving that the fluctuations originate in the outer shear layer of the vortex, not in the core.

INTRODUCTION

This paper demonstrates the use of surface mini-fences to reduce the intensity of narrow-band velocity fluctuations that exist in the vortical flow over moderately-swept wing configurations at angle of attack. A series of experiments[1] has shown the phenomenon to be common to models of existing combat aircraft, generic high-speed aircraft at angle of attack, and to isolated delta wings. After ruling out various hypotheses about the origin of these fluctuations, we have traced this origin to counter-rotating structures, oriented along helical trajectories (nearly spanwise) near the wing surface. These appear to be consistent with a centrifugal type of instability[2].

Ref. 1 provides a summary of previous work and the systematic examination of various hypotheses regarding the drivers of tail buffeting on moderately-swept aircraft configurations. Ref. 3 reports initial efforts to modify the fluctuation spectra by following the above observations of counter-rotating structures. As shown in Fig. 1, small fences were placed at various positions and orientations along the wing surface. Fig. 2 shows that the lift and drag characteristics were virtually unaffected. Fig. 3 shows the accompanying changes in the spectrum of velocity fluctuations measured at a location corresponding to the approximate top of the vertical tail. Both attenuation and amplification were demonstrated, as seen in Fig. 3. Fences placed along rays of the delta wing (type B) were the most successful in attenuating the spectral peak, whereas spanwise fences (type D) amplified the peak. The attenuation at the peak is not accompanied by any increase in intensity at other frequencies, so a net attenuation of fluctuation energy is achieved. Hubner[3] also mapped out the contours of attenuation in a cross-flow plane at the wing trailing edge to ensure that the devices were not merely shifting the vortex flow pattern. This work formed the basis for the present effort. In this paper, we report further experiments to optimize the attenuation and reduce the size of the devices required. Then we use active devices, where the effects of deployment height and duty cycle are used to draw further conclusions about the phenomenon.

Objectives

The objectives are to:
1) identify the most effective passive fence position and orientation for maximum attenuation of peak intensity,
2) determine the effects of fence height, length and multi-fence combinations on attenuation, and
3) test various active fence designs to see if a more effective tuned response can be obtained.

EXPERIMENTS

The experiments were performed in the 42" x 42" open-return wind tunnel at the School of Aerospace Engineering. The turbulence intensity is under 0.3 %. A single-sensor hot film probe was positioned with a three-component traverse. The sensor was placed perpendicular to the freestream direction so that it was

*: USAF Senior Knight. Student Member, AIAA.
†: Graduate Research Asst. Student Member, AIAA.
‡: Professor. Associate Fellow, AIAA.

equally sensitive to both vertical and streamwise velocity and less sensitive to lateral velocity. The anemometer signal was digitized using a 16-bit, multichannel, sample-and-hold analog-digital converter. One channel received the full hot-film signal, and a second channel received a high-pass-filtered (0.1 Hz) amplified hot-film signal. The signal was monitored on an oscilloscope, and the amplification was adjusted between 1 and 100 to optimize digitizing accuracy.

For each test case, 50 sample blocks were used to calculate a stable ensemble averaged autospectrum for each signal. There were 512 data points taken per sample block, and the Nyquist frequency was 256 Hz. These values were chosen to achieve a frequency resolution of 1 Hz. The spectra showed that there was little signal beyond 200 Hz.

The cropped delta-wing with 18 deg. beveled edges (Fig. 4) had 59.3° leading edge sweep, and a root chord of 398 mm. For all tests reported, the angle of attack of the model was fixed at 25°. The model was held by a vertical mount fastened to the under-side with counter-sunk screws through the upper surface, to ensure the upper surface flow was unaffected.

Passive Fence Geometry

Static fences were first shown by Hubner[3] to be beneficial in modifying the fluctuations measured near the vertical tail position. This experiment investigated the effects of fence length, height and location. Fence lengths were varied between 6.4 mm and 50.8 mm, and heights between 1 and 10 mm. Fences were also moved incrementally from the trailing edge forward along three rays from the apex, β=18°, 22.5° and 28.2°. Fences were tested aligned with these rays and aligned parallel with the model center line. Spectral data were taken using a hot-film anemometer located at the approximate position of a vertical twin-tail. In a body fixed coordinate system with origin at the apex of the model, this Probe Position A is <x,y,z> = <338 mm, -75.6 mm, 103 mm>. Fig. 4 shows the location of Probe Position A and Fence Position A.

Active Fences

The actuator used to oscillate the fence was a 20 volt solenoid, shown in Fig. 5. Activating the solenoid raise the fence through a slot in the wing surface, against a spring. It was mounted below the bottom surface of the wing on a stand separate from that supporting the model, as seen in Fig. 6. The solenoid and plunger below the model were enclosed in a sealed shroud to minimize flow interference. The fence was made from a 0.61 mm thick aluminum plate. It passed through a 1.02 mm wide and 55 mm long slot machined in the model. The fence mean height above the upper surface was adjustable using set screws in the mounting stand. A fence height oscillation amplitude of 1 mm was driven by a 20V square-wave applied to the solenoid. The frequency of the oscillation was varied between 10 and 60 Hz.

The velocity spectrum was measured without fence deployment at six locations 12.7 mm above the surface of the model. As measured from the apex down the β=16.5° ray, the foremost position was at 169 mm (10 mm inboard of the Fence Position A midchord). Each subsequent point was 40 mm further down the β ray. The final point ended at the b'/b=1 line. The probe was moved to Probe Position A and various heights of static fences tested. Fences of various heights oscillating over the entire range of frequencies were tested. Finally, an active ramp device was also tested.

RESULTS

Spectral Attenuation

One of our objectives was to minimize the fence length and height. For all the fences tested there is a region over the wing where attenuation is achieved. As shown in Fig. 7, this region is bounded by the b'/b=0.2 and b'/b=0.8 streamwise stations and the β=18° and β=28.2° chordwise stations. Fig. 8 shows an example of the effect of a static fence at Fence Position A on the velocity spectrum at Probe Position A (with V_∞=6.1 m/s). The spectral shape is modified slightly over most of the frequency range, but a large attenuation of spectral energy level is obtained. There is a minor shift in the location of the spectral peak, from 24 Hz for the fence-off case and at 34 Hz for the fence-on case. This is seen to be primarily because the attenuation at 34 Hz is not as great as that at 24 Hz.

Fence Location

Fig. 7 shows the test results for a series of 3 mm x 50 mm fences placed at different locations on the model's surface. These tests were conducted with the model at 25° angle of attack and a freestream speed of 12.2 m/s. The figure shows fence positions and percent spectral peak reductions achieved. Fence locations for only one half of the model are pictured, though in each test two fences were placed symmetrically about the center line. The fences were placed with their leading edge on a β-line and aligned parallel with the model center line as indicated in the figure. As mentioned previously, various fence lengths and orientations were tested, but only the most effective are presented here. The best attenuation was achieved with a 3 mm x 50.8 mm fence positioned with it's leading-edge at <x,y,z> = <13.90 cm, 5.77 cm, 0 cm> and aligned parallel with the model center-line. This fence position, as seen in Fig. 7, attenuates the peak in the velocity spectra by 71%; which is the best attenuation for all the positions and orientations tested. For this reason, this position was defined as Fence Position A. At this same position, a preliminary fence height test showed that a 6 mm x

50.8 mm fence produced an even greater 78% attenuation. This result is seen in Fig. 9.

Fence Height Effect

Taking Fence Position A as the optimal fence location and orientation for the model at 25 deg. angle of attack, the effect of fence height was determined. Fig. 10 shows the effect of fence height on spectral peak intensity for three freestream speeds. Fence heights below 1 mm show no conclusive reductions. Above 6 mm, additional fence height has little effect in reducing the peak spectral intensity. This figure shows two important features of the structures responsible for the narrow-band fluctuations. ***First, they are not confined to the boundary layer. Secondly, they do not originate in the core or central region of the vortex flow.*** Both findings are consistent with our finding of spanwise-oriented, counter-rotating structures of the Görtler type.

Percentage Reductions

From Fig. 9, the percentage reduction in spectral intensity for the fence-on case is calculated (from Fig. 10) in the frequency interval corresponding to the peak spectral level (proportional to the square of the velocity fluctuation amplitude in that frequency interval). Since the peak is different for the fence-off and fence-on cases, the reduction is thus underestimated. For example, the spectral level at 24 Hz in the fence-on case is considerably lower than that at 34 Hz. This conservative criterion was considered appropriate to produce conservative estimates of the possible tail buffet reductions and improvements in fatigue life.

Figure 9 shows the percent reductions between the fence-off and fence-on cases shown in Fig. 10, where the fence height effects are seen. For fence heights between 1 mm and 6 mm, fence effectiveness dramatically increases. For the cases presented in this figure, fence effectiveness increases slightly with freestream speed. The two points at 12.2 m/s show a very high level of attenuation.

Active Fences

As seen in the static fence tests, fences placed on the surface of the model near the origin of the narrow-band fluctuations can attenuate the spectral intensity of the fluctuations. We attempted to force the fluctuation structures at frequencies corresponding to their passage, in an attempt to explore possible resonance or suppression by phase-cancellation. Because the frequency of the spectral peak decreases downstream, the frequency at Probe Position A is lower than that at Fence Position A. Velocity spectra measured 12.5 mm above the model surface along the β=16.5° ray revealed higher frequencies near the apex, dropping off to a nearly constant value near the trailing edge. This can be seen in Fig. 11 for a freestream velocity of 4.57 m/s. At the furthest upstream position, near the center of Fence Position A, the spectral peak was at 41 Hz. At a probe height of 3.18 mm above the same location, a frequency of 58 Hz was measured. These data led to the design of a fence capable of oscillating at frequencies up to 60 Hz. The same trend in frequencies was observed at two higher tunnel speeds, with higher frequencies at each location. Due to the frequency limitations of the solenoid being used, we decided to use the tunnel speed of 4.57 m/s.

The oscillating fence was at Fence Position A. Testing of the oscillating fences produced a similar trend in reduction of peak intensity as a function of fence height. Fig. 12 shows peak intensity data for three different fence heights and frequencies ranging from 0 to 60 Hz. In all cases the fence oscillation had an amplitude of 1 mm, so the data labeled as '1 mm' refers to a fence oscillating between 0 (flush with the upper surface of the model) and 2 mm. In none of the three cases does it appear that oscillating the fence has a beneficial effect over the static fences. Averaging over all frequencies, the effect of an oscillating fence is very similar to that of a static fence with height equal to the mean height of the oscillating fence. Additional tests were performed with a static and dynamic ramp device which was used to introduce vorticity aligned normal to the local flow near Fence Position A. This too had no benefit over the static fences.

DISCUSSION

The work in this paper was initially undertaken as an exercise in a Flow Control course, with the primary objective of seeing if an active device could produce either resonance or phase-cancellation effect far beyond that observed with the static fences. It led to a very different set of findings. The active fence experiments showed that the structures generating the narrow-band fluctuations are very stable and repeatable: periodic perturbation, attempted over a wide range of frequencies in the vicinity of the spectral peak, showed little effect beyond the duty-cycle effect of static fences. This would appear to be further evidence against "hydrodynamic instability" types of hypotheses for the origin and amplification of these fluctuations.

The static fence results are equally significant. The effect of fence height shows that:

a) this is not a boundary layer phenomenon: obstructing only the boundary layer has little effect,

b) this is not a core-generated vortex instability: extending these fences far into the core (or center of the post-burst) flow has no more effect than the 6 mm extension, and

c) obstructing the shear region at the outer edge of the vortex flow, above the surface, has a dramatic effect, is very repeatable, and clearly depends on fence height across this region.

Once again, the centrifugal-type instability which we proposed in Refs. 2 and 4 is seen to be consistent with the observations. The post-burst vortex over highly-swept wings (F/A-18, for example), or the vortex flow over moderately-swept wings (F-15 and other aircraft) at above 20 deg. angle of attack, where no un-burst region is seen, exhibits a radial profile of tangential velocity which resembles solid-body rotation. At the outer edge of this region, there exists a sharp decay of tangential velocity, where the decay is steeper than the 1/r decay outside the core of a strong vortex. This region, then, is ripe for the generation of centrifugal instability, as predicted by Rayleigh's second theorem on the stability of velocity profiles (Ref. 5). The presence of the solid surface and its boundary layer immediately below the vortex further enhances this Görtler-type instability, and amplifies the counter-rotating structures. The propagation of these structures follows a helical trajectory, as may be expected from the helical nature of the vortex flow. The lowering of frequency downstream, and the amplification of the velocity disturbance, are consistent again with the conical shape of the vortex flow.

Large fences have been used on the F-15 (Ref. 6) and on the F/A-18 to reduce tail buffeting. On the F/A-18, the vortex trajectory and burst location are substantially modified. On the F-15, hot-film spectral intensity appears to have been modified somewhat by very large fences placed far out along the span in an attempt to control the spanwise flow along the wings. These appear to have been abandoned because of the high penalties in weight and performance.

The success of our mini-fences oriented along rays or the freestream direction in the region of origin of these structures indicates that a tailored deployment scheme can suppress the narrow-band fluctuations by a large percentage, enough to change the narrow-band spectrum to a broad-band, low-intensity fluctuation. This is done with negligible impact on the aerodynamic performance of the wing, and deployable versions may be easily designed for high-angle-of-attack operation over a range of angles of attack. The efficiency of the devices appears to increase with flow velocity, as may be expected from the greater strength of the disturbance structures relative to freestream turbulence; this needs further investigation.

CONCLUSIONS

The use of small vertical fences placed at strategic locations is seen to be effective in attenuating narrow-band velocity fluctuations over a 59.3 deg. delta wing at 25 deg. angle of attack. Experiments to determine optimal fence locations, orientations, and the effect of a vertical oscillation of the fence produced the following conclusions:

1. Two symmetrically placed 6 mm x 50.8 mm fences positioned beginning at <x,y,z> = <13.90 cm, +/-5.77 cm, 0 cm> and aligned parallel with the model center-line attenuate the peak in the velocity spectra by as much as 78%.
2. A variety of multiple fence combinations were tried, but attenuation did not exceed that of the 6 mm x 50.8 mm static fence.
3. Fence height had little effect below 1 mm, and little additional effect beyond 6 mm. This suggests that the narrow region between the outer edge of the burst-vortex flowfield and the surface boundary layer is responsible for the fluctuations, as opposed to instabilities of the core or the post-breakdown central region of the vortex flow.
4. Exciting the fence over the frequency range of the narrow-band fluctuation produced no visible tuning or phase-cancellation effects: the attenuation results appear to correspond to the duty cycle of the fence deployment height.
5. The attenuation results provide further strong evidence of the centrifugal-instability model of the narrow-band fluctuations.

ACKNOWLEDGMENTS

This work was performed under support from the Air Force Office of Scientific Research (Major Dan Fant and Dr. Len Sakell), and the National Science Foundation Leadership in Laboratory Development Program. The Air Force Palace Knight program supports the graduate research of Mr. Klein. Mr. Lentz's participation was enabled through AE8143, a Flow Control Elective course developed using NSF support. Special thanks are given to the students in the Experimental Aerodynamics Group who assisted with the research.

REFERENCES

1. Komerath, N. M and Hubner, J. P., "Narrow-Band Fluctuations in Vortex Flows," AIAA 95-2304, June 1995.
2. Hubner, J. P. and Komerath, N. M., "Counter Rotating Structures Over a Delta Wing,". *AIAA Journal*, September 1996.
3. Hubner, J. P. and Komerath, N. M., "Modification of Spectral Characteristics in a Vortex Flow Field," AIAA 95-1795, June 1995.
4. Hubner, J. P. and Komerath, N. M., "Visualization of Quasi-Periodic Structures in a Vortex Flow," AIAA 94-0624, Jan. 1994.
5. Schlichting, Hermann, Boundary-Layer Theory, McGraw-Hill, New York, 7th ed., 1979.
6. Colvin, B. J., Mullans, R. E., Paul, R. J., and Roos, H. N., "F-15 Vertical Tail Vibration Investigations," MDC Report A6114, McDonnell Aircraft Co., St. Louis, MO, Sept. 1979.

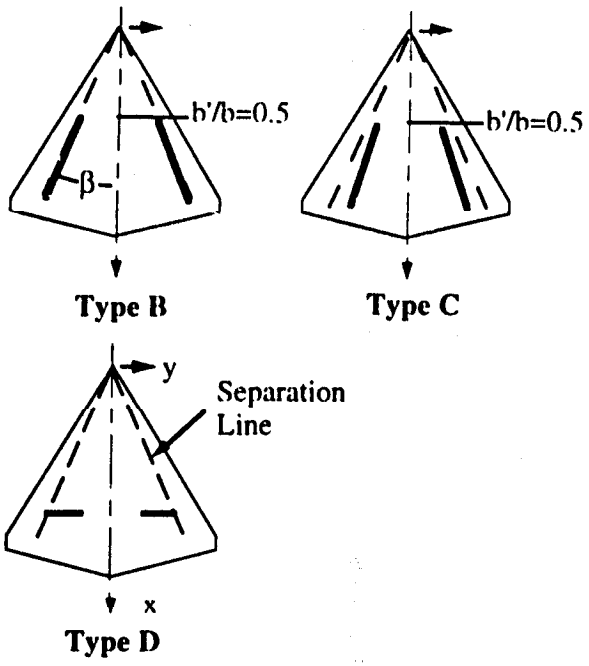

Figure 1 Surface fence orientations used in velocity spectra modifications (Ref. 1).

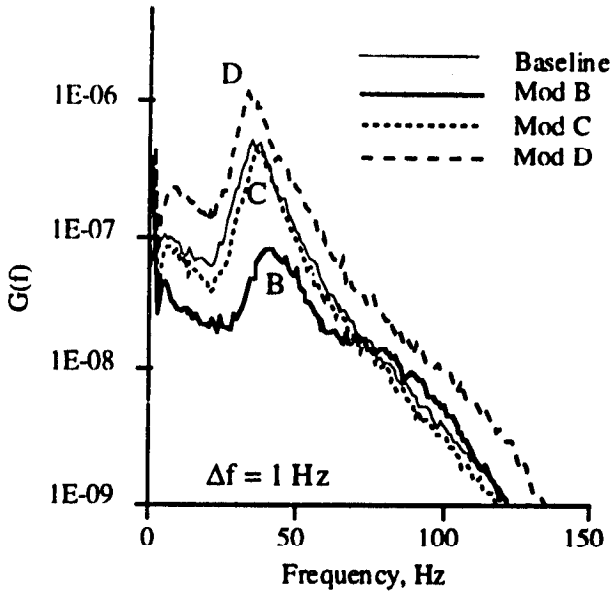

Figure 3 Initial spectra modification results for the 59.3° delta wing, where G(f) is a nondimensional autospectra intensity function (Ref. 1).

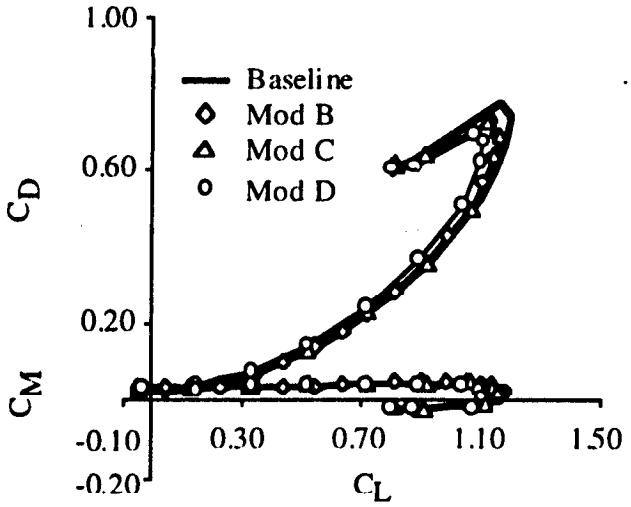

Figure 2 Drag and pitching moment polars for the 59.3° delta wing (Ref. 1).

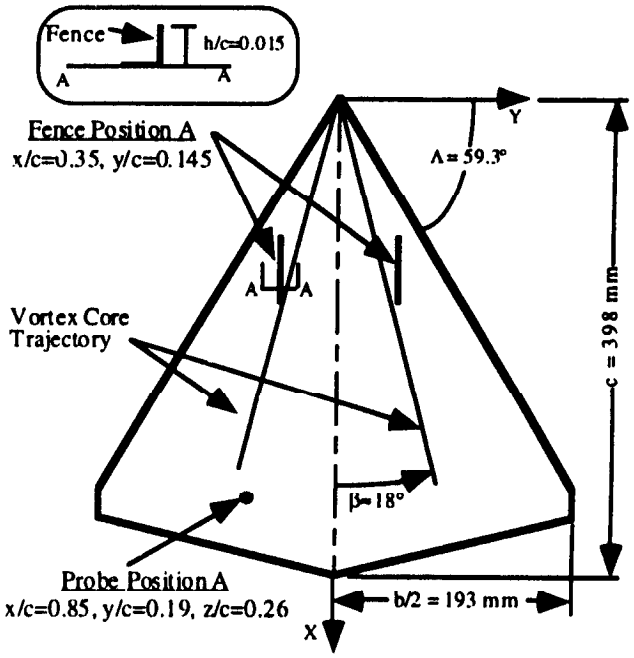

Figure 4 Diagram of fence placement and general vortex core trajectory.

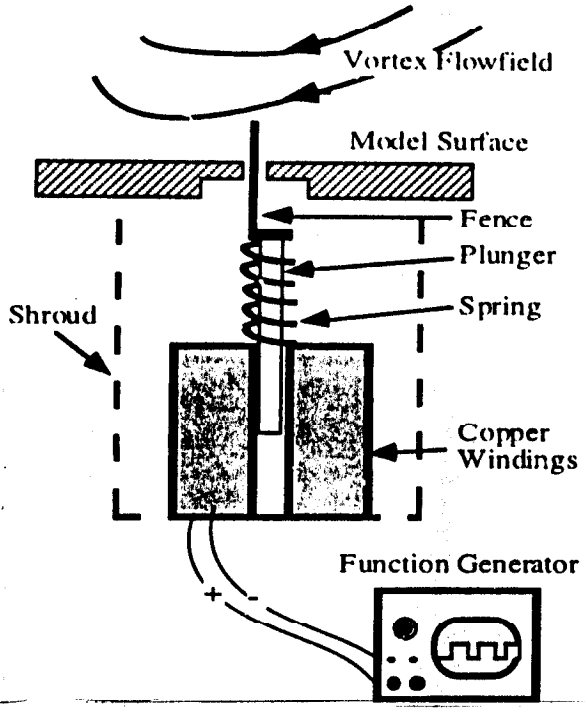

Figure 5 Schematic of 20 V solenoid active fence system.

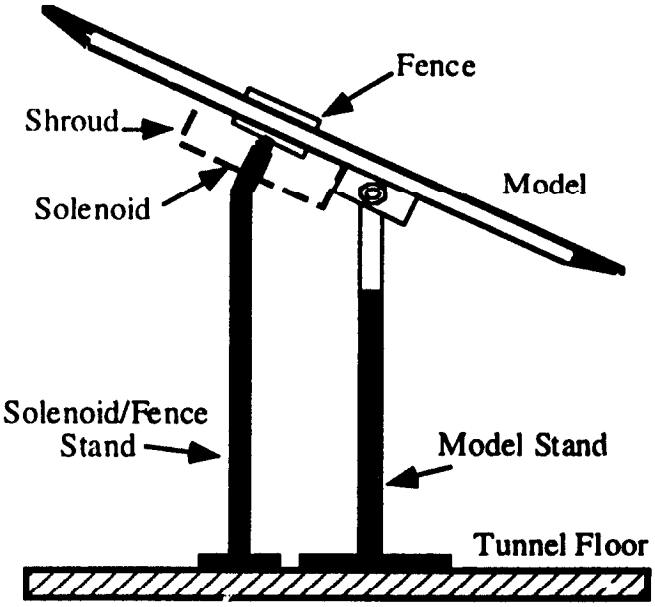

Figure 6 Isolation method for active fence to reduce vibrations on the model.

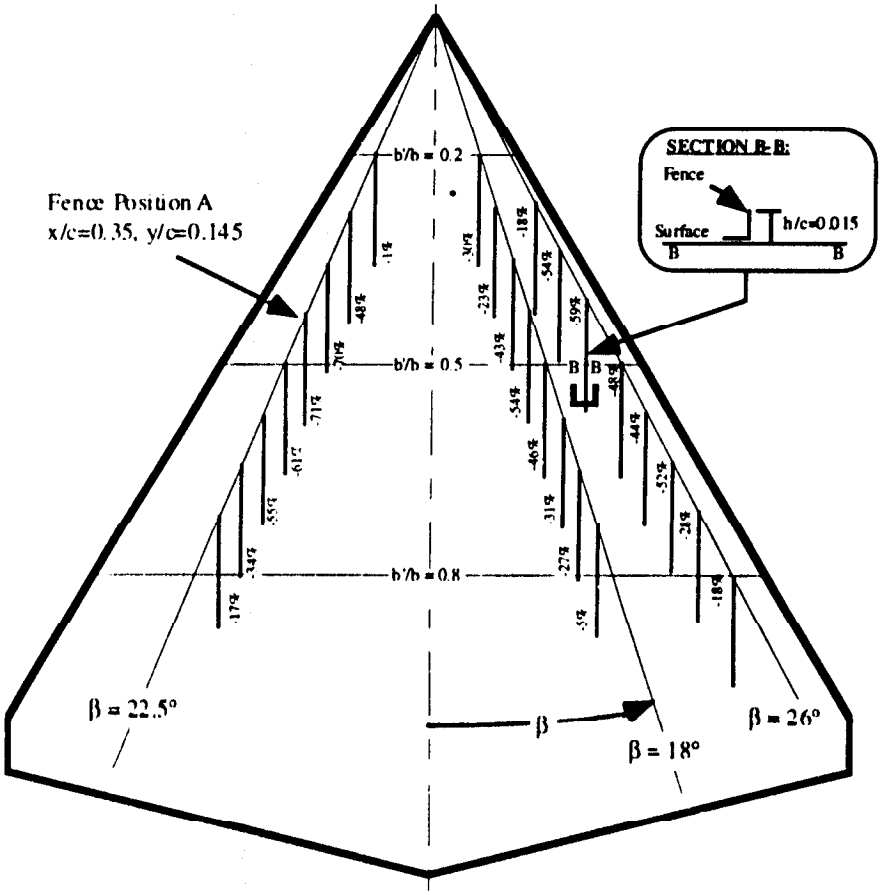

Figure 7 Fence placement and percent reductions in spectral peak intensity (V_∞ = 12.2 m/s).

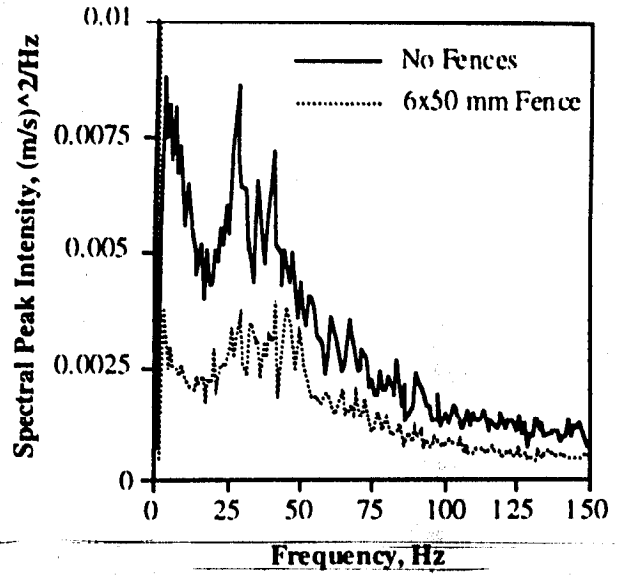

Figure 8 Spectra comparison with fence-off and fence-on at Fence Position A.

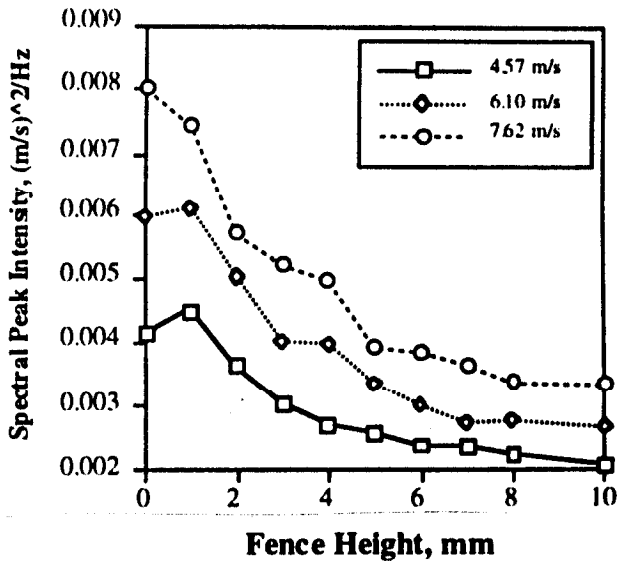

Figure 10 Effect of fence height on spectral peak intensity for three freestream velocities.

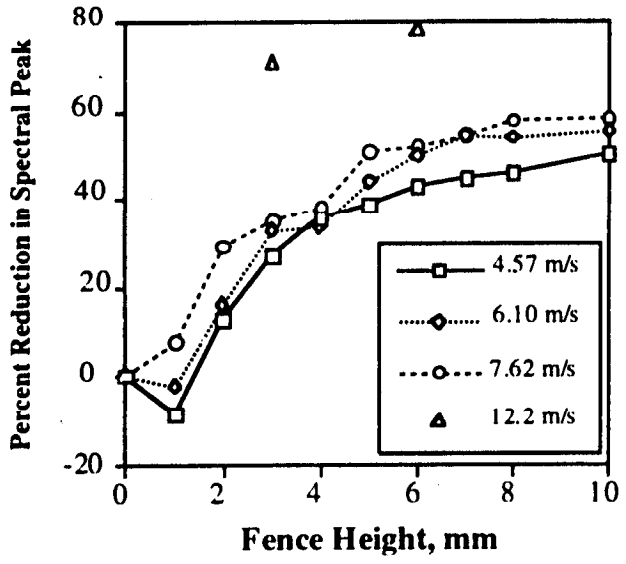

Figure 9 Percent reduction in spectral peak intensity with increasing fence height at Fence Position A.

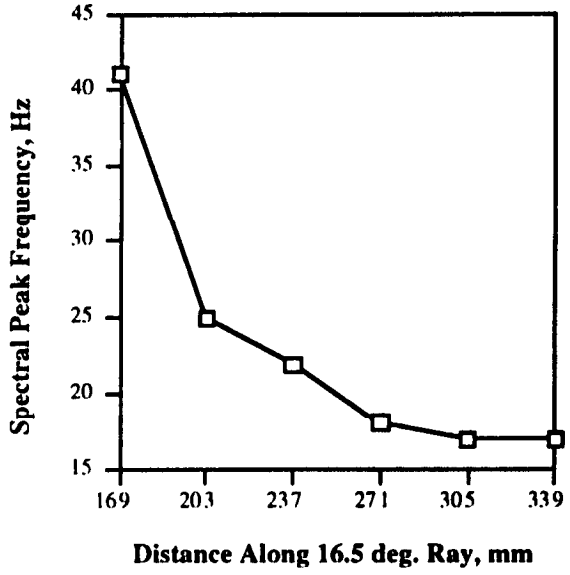

Figure 11 Near surface spectral peak frequency verses downstream distance, measured along the β=16.5° ray from the apex of the model.

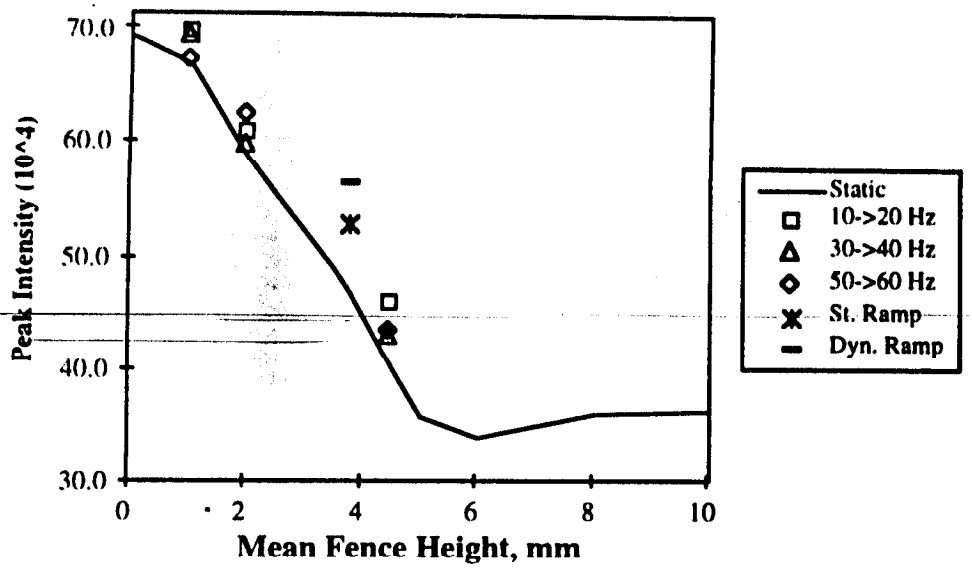

Figure 12 Mean height comparison of dynamic fence with static fence and dynamic ramp.